# Simulation of interstitial diffusion in graphite

Yuchen Ma*
*Laboratory of Physics, Helsinki University of Technology, P.O. Box 1100, Helsinki 02015, Finland and Fachbereich Physik, Universität Osnabrück, D-49069 Osnabrück, Germany*
(Received 5 February 2007; revised manuscript received 22 June 2007; published 15 August 2007)

First-principles method based on the density-functional theory is used to study the diffusion of the single carbon interstitial in graphite. Possible diffusion processes in directions both parallel and perpendicular to the basal plane are analyzed. A different path for the interstitial to penetrate the graphitic layer is proposed. Along this path, the migration is carried out through atom exchange between the interstitial and the lattice atom, with a barrier lower than 0.5 eV. Introducing shear into the graphite may reduce the interstitial migration energy.

DOI: 10.1103/PhysRevB.76.075419 PACS number(s): 61.80.Az, 61.72.Ji, 81.05.Uw

## I. INTRODUCTION

Irradiation method has become an effective way to modify the properties of materials. Electron irradiation of graphite could produce carbon onions and induce nucleation and growth of diamond inside the carbon onions.[1,2] Electron irradiation of multiwalled carbon nanotubes can cause large pressure within the nanotube cores that can plastically destroy solid materials encapsulated inside the core.[3] Irradiation effects in graphite are also important for dimensional changes and defect rearrangements in the nuclear reactor. The behavior of defects is of great relevance to the study of the irradiation effects. Determination of the mechanism for the atomic motion in the graphite is also important for the understanding of the growth process of carbon nanotubes.

A large number of experiments have been performed to study the behavior of defects in graphite and carbon nanotubes.[1,4–10] The single interstitial is expected to be highly mobile along the *a* axis of graphite, with the migration energy less than 0.3 eV.[1,7,8] Theoretical calculations predicted the migration energy to be less than 0.03 eV (Ref. 11) in graphite and to be 0.4 eV on a graphene sheet[12] along the *a* axis. However, the knowledge of diffusion along the *c* axis is still rare. No direct experimental data have been obtained yet. The general idea is that the interstitial diffusion along the *c* axis is inhibited due to the very high activation energy (>5 eV) of mobility required. By the tight-binding technique, Xu *et al.* estimated that the migration energy along the *c* axis was larger than 2.3 eV.[11] Thrower and Mayer[13] gave an argument two decades ago that the interstitial diffusion in the graphite was isotropic, which seems unbelievable considering the anisotropic lattice structure of the graphite. Following experiments and theoretical calculations[11] disproved this argument. The most controversial point is the possible diffusion path along the *c* axis.[1] In this paper, an interstitial diffusion path along the *c* axis is proposed. Along this path, the energy required to penetrate the basal plane is less than 0.5 eV. This value is close to the single-interstitial migration energy (0.3 eV) along the *a* axis obtained from the recent experiments.[7,8] Recent density-functional theory (DFT) calculations[14] proposed a much higher interstitial migration energy (>1.5 eV) along the *a* axis. We also performed a thorough study on the interstitial diffusion along the *a* axis, trying to solve the contradiction between this theoretical calculation and the experiments.

DFT is a good selection to perform a large number of calculations with high accuracy and high efficiency. However, the main deficiency of DFT in graphite is that it fails to describe the long-range van der Waals (vdW) interactions within both the local density approximation (LDA) and the generalized-gradient approximation (GGA). LDA could calculate very well the *c*-axis lattice constant of graphite, but usually overestimates the binding energy.[15] This overestimation of the binding energy can be reduced by using GGA. However, GGA leads to a strong reduction of the interlayer bond and an expansion of the axial ratio to $c/a=1.8$.[16] To date, two methods have been proposed to overcome this deficiency. One is to derive suitable exchange-correlation functionals for DFT which could describe the vdW interaction correctly.[17] This method is quite CPU time consuming. The other method is to combine the empirical method based on the Lennard-Jones potential and the *ab initio* DFT-GGA calculation. This kind of combination has been successfully used to study graphite,[15] biological molecules,[18–20] and carbon nanotubes.[21] To test our results from DFT-GGA, some calculations have been repeated by the second method, i.e., by a vdW-corrected DFT-GGA (vdW+DFT-GGA) approach which is own-developed based on the VASP code.[22,23]

## II. THEORY AND METHODS

The DFT calculations have been performed using the periodic plane wave basis VASP code,[22,23] implementing the GGA of Perdew and Wang.[24] The projected augmented wave potential[25,26] is used to describe the core ($1s2$) electrons. A kinetic energy of 400 eV was found to converge the total energies of the systems to within meV. For vdw+DFT-GGA, a vdW term $E_{vdW}$ is introduced to obtain the total energy of the system $E_{tot}=E_{DFT}+E_{vdW}$, where

$$E_{vdW}=-\sum_{i<j} f(R_{ij})\frac{C_6^{ij}}{R_{ij}^6}. \quad (1)$$

$R_{ij}$ is the distance between atoms $i$ and $j$, and $C_6^{ij}$ and $f(R_{ij})$ are the interaction coefficient and the related damping function.[18–20]

For a graphene sheet, DFT-GGA gives the lattice constant $a_0$ of 2.47 Å. For bulk graphite, GGA gives the lattice constant $c_0$ around 9.0 Å and the interlayer binding energy less

 

TABLE I. Results of calculations in various approximations for the equilibrium lattice constants ($a_0$, $c_0$), total cohesive energy ($E_c$), interlayer binding energy ($\Delta E_c$), and $c$-axis elastic constant ($c_{33}$) of graphite with *ABAB* stacking and their comparisons with experiments.

| | $a_0$ (Å) | $c_0$ (Å) | $E_c$ (eV/atom) | $\Delta E_c$ (eV/atom) | $c_{33}$ (GPa) |
|---|---|---|---|---|---|
| LDA[a] | 2.44 | 6.64 | 8.90 | 27 | 30.4 |
| GGA[b] | 2.47 | ~9.0 | 8.02 | ~2 | ~0.7 |
| vdw+GGA[b] | 2.47 | 6.6 | 8.08 | 63 | 62 |
| Expt. | 2.46[c] | 6.70[c] | 7.37[d] | 43[e] $35^{+15}_{-10}$[f] $52\pm5$[h] | 36.5[g] |

[a]Reference 15.
[b]This work.
[c]Reference 27.
[d]L. Brewer (unpublished) (as cited in Ref. 28).
[e]Reference 15.
[f]Reference 29.
[g]Reference 31.
[h]Reference 30.

than 2 meV/atom, both of which deviate from the experimental values (see Table I). Since the vdW interaction is much weaker than the in-plane interatomic bond energy, the influence of the vdW interaction on the in-plane lattice constant could be neglected. By fixing the in-plane lattice constant $a_0$ at the value obtained from the graphene sheet (2.47 Å), the lattice constant $c_0$, interlayer binding energy, and $c$-axis elastic constant ($c_{33}$) are calculated to be 6.6 Å, 63 meV/atom, and 62 GPa by vdW+DFT-GGA, respectively, which are in reasonable agreement with the experiments[15,29,30] (see Table I and Fig. 1).

We construct $5\times5$ supercells in the in-plane direction of graphite. The cell containing a graphene sheet has enough gap in the $c$-axis direction so that the interaction between adjacent images is negligible. For the study of the interstitial in graphite, two kinds of supercell models are used such as model I and model II shown in Figs. 2(a) and 2(b), respectively. These two models have the *AB*-stacking order. In both models, the position of some corner atoms in the supercells are fixed during the relaxation so that the planes could not move with respect to each other in both the $a$-axis and $c$-axis directions. For a better comparison between DFT-GGA and vdW+DFT-GGA calculations and a better comparison with the experimental results, the distance between graphite layers in the supercell is set to the experimental value of 3.4 Å. In model I, there is a large gap in the supercell along the $c$ axis to prevent interaction between adjacent images. In model II, the length of the supercell along the $c$ axis is set to 6.8 Å, i.e., to simulate *ABAB*… bulk graphite. These two models represent two extreme cases, the one where the adjacent supercells have no influence (model I) and the one where the adjacent supercells have the strongest influence (model II). In reality, interstitials in graphite will sit in the environment between these two extrema. To test the convergence of the formation energy with respect to the size of the supercell, a

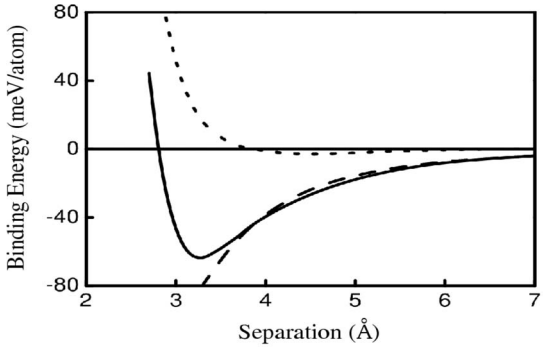


FIG. 1. Interlayer separation dependence of the interlayer binding energy obtained by the *ab initio* DFT-GGA calculation (dotted line) and by the vdW-corrected DFT-GGA calculation (solid line). The dashed line is the vdW contribution given by Eq. (1). The in-plane lattice constant is fixed at 2.47 Å.

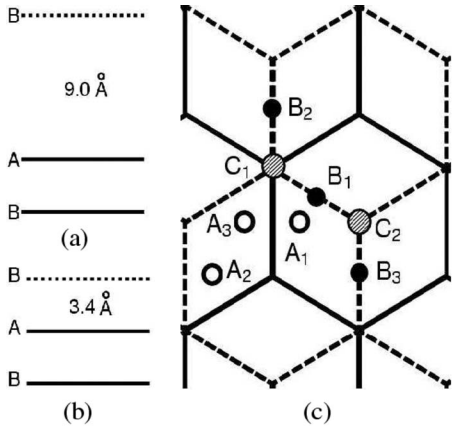


FIG. 2. (a) and (b) show the two kinds of supercells, model I and model II, respectively, used in the calculations. The solid lines denoted by A and B are in a supercell, while the dotted lines denoted by B belong to the adjacent supercell. In (c), $A_i$, $B_i$, and $C_i$ ($i=1$, 2, and 3) are possible interstitial sites. Solid and dashed lines represent upper and lower basal planes, respectively.

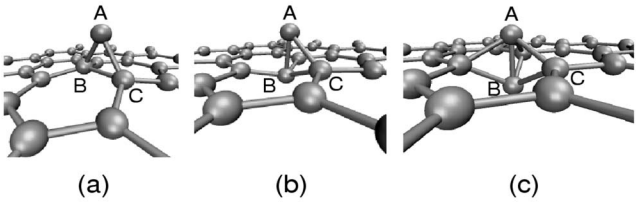


FIG. 3. Migration process of a carbon adatom (A) penetrating a graphene sheet by atom exchange with the lattice carbon atom B. (a) and (c) are the ground state and the metastable state, respectively. (b) is the highest-energy state along the migration path.

$6\times6$ supercell is constructed. The formation energies calculated by DFT-GGA are converged to within 0.1 eV. The error in the migration energy introduced by the small $5\times5$ supercell is less than 0.1 eV as discussed below. The minima of the total energy are found using a conjugate gradient algorithm. The migration path between different minimum-energy configurations is calculated by the nudged elastic band method[32] implemented in VASP. The data presented below are calculated based on the $5\times5$ supercell if not explicitly stated otherwise.

## III. RESULTS AND DISCUSSION

### A. On the graphene sheet

First the properties of a carbon adatom adsorbed on a graphene sheet are studied by DFT-GGA. The experiment[5] and theoretical calculations[12] have proven that the C adatom prefers to form a bridgelike structure on the graphene surface [Fig. 3(a)]. The migration barrier on the surface is calculated to be 0.4 eV.[12] Apart from this lowest-energy state, a metastable state is found as shown in Fig. 3(c). In this state, adatom A pushes one lattice atom (B) out of the graphene plane, forming a symmetric structure. Both atoms A and B form three bonds with the graphene plane at the length of 1.56 Å. The distance between atoms A and B is 1.58 Å. The formation energy of this metastable state is 7.0 eV, 0.5 eV higher than that of the ground state [Fig. 3(a)]. The migration barrier from the ground state to the metastable state is 0.9 eV. Figure 3(b) shows the highest-energy state along the migration path. Through this migration path, the carbon adatom may penetrate the graphene sheet with much lower energy than expected before.[1,11] Starting from the ground state, when the system temperature was raised gradually, the above migration process could occur at around 800 K. In bulk graphite, the presence of adjacent layers may lower the barrier further, which will be discussed below.

### B. In the graphite

There are many possible configurations for the interstitials in bulk graphite.[14] In my calculations, three stable structures are found, as shown in Fig. 4. In this paper, the structures shown in Figs. 4(a)–4(c) are denoted as A, B, and C, respectively. In structure A, the interstitial forms two bonds with each graphite layer. Structures B and C are similar to the structures of an adatom on a graphene sheet, as shown in Figs. 3(a) and 3(c), respectively. Structure C could be further

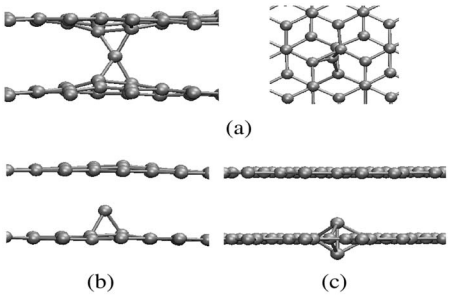


FIG. 4. Three possible interstitial positions in the *AB*-stacking graphite. In this paper, the structures in (a), (b), and (c) are denoted as A, B, and C, respectively. (a) shows the side view (left) and the top view (right) of structure A.

classified into two inequivalent structures C1 and C2 [Fig. 2(c)]. In structure C1, the interstitial sits between the hexagon vertex points of two adjacent layers, while in structure C2, the interstitial sits between the hexagon vertex point in the lower layer and the hexagon center in the upper layer. Table II presents the formation energies of these three structures in model I and model II calculated by DFT-GGA and vdW+DFT-GGA, respectively.

Both structures B and C induce hillocks in graphite. Structure C induces much less strain in graphite than structure B. So in model I by DFT-GGA, the energy difference between structures B and C decreases to 0.1 eV for C1 and 0.2 eV for C2, respectively, which are much less than those on a graphene sheet. In model II by DFT-GGA, the graphite layers in the adjacent supercells exert strong repulsive force on the hillock and try to compress it. The compression in structure B is heavier than that in structure C. The energy of structure C1 becomes lower than that of structure B. Contrary to model I by DFT-GGA, the energy of structure C is lower than that the structure B in model I by vdW+DFT-GGA. In model II by vdW+DFT-GGA, both the energy sequence and the energy difference between the four kinds of structures are the same as those in model II by DFT-GGA.

In the following discussion, the notation in Fig. 2(c) will be used for different structures. We first study the migration from A1 to C1 (the migration from A1 to C2 has a similar process), which is not only related to the diffusion along the *a* axis, but also related to the diffusion along the *c* axis. In all the two models, to reach C1 from A1, the interstitial must pass B1, i.e., B1 is the necessary transition state. Figures

TABLE II. Formation energies (eV) of interstitials at positions A, B, C1, and C2 in the supercell model I (M I) and model II (M II) calculated by DFT-GGA (second and third columns) and vdW+DFT−GGA (fourth and fifth columns).

| | M I-DFT | M II-DFT | M I-vdW | M II-vdW |
|---|---|---|---|---|
| A | 6.4 | 6.4 | 6.2 | 6.3 |
| B | 6.9 | 7.5 | 7.4 | 7.4 |
| C1 | 7.0 | 7.4 | 7.0 | 7.3 |
| C2 | 7.1 | 7.5 | 7.1 | 7.4 |

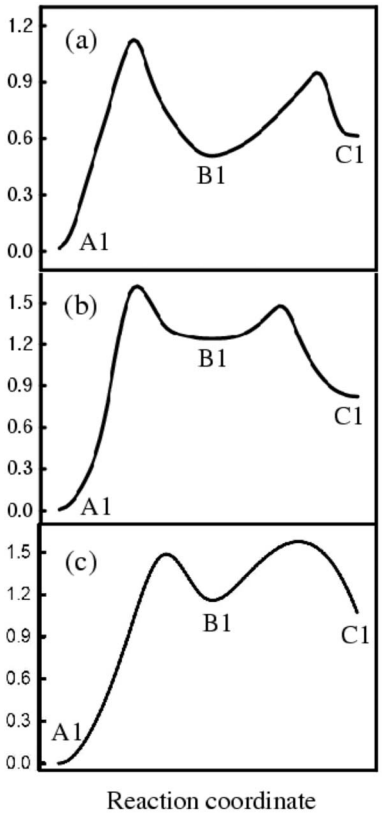


FIG. 5. Energy profiles for the interstitial diffusion from positions A1 to B1 to C1 denoted in Fig. 2(c). (a) and (b) are obtained from calculations by DFT-GGA and vdW+DFT-GGA, respectively, using the supercell model I. (c) is obtained from calculations by DFT-GGA using the supercell model II.

5(a)–5(c) show the energy profiles along the migration path A1→B1→C1 calculated by model I with DFT-GGA, model I with vdW+DFT-GGA, and model II with DFT-GGA (the energy profile calculated by model II with vdW+DFT-GGA is nearly identical to that by model II with DFT-GGA), respectively. The barrier from A1 to B1 is in the range of 1.2–1.7 eV, while the barrier from B1 to C1 is less than 0.5 eV. Due to the presence of adjacent graphite layers, the barrier from B1 to C1 is less than the barrier (0.9 eV) for the similar process on a graphene sheet (Fig. 3). This means that penetrating the graphite layer through atom exchange is easier in bulk graphite. In model II with DFT-GGA, the barrier from A1 to B1 in the $6\times6$ supercell is 0.07 eV higher than that in the $5\times5$ supercell, while the barrier from B1 to C1 in the former is 0.02 eV lower than that in the latter. This proves that the $5\times5$ supercell is large enough to study the diffusion of the single interstitial in graphite.

We come to the conclusion that the migration of the interstitial along the $c$ axis is along the path $B_i\rightarrow A_i\rightarrow B_i\rightarrow C_i\rightarrow B_i\ldots$. Migration along the $c$ axis is composed of two parts, the interlayer migration ($B_i\rightarrow A_i\rightarrow B_i$) and the intralayer migration ($B_i\rightarrow C_i\rightarrow B_i$). In the *AB*-stacking graphite, the total interstitial migration barrier along the $c$ axis is in the range of 1.2–1.7 eV, which is determined by the interlayer migration. This value is much less than the value expected before (>2.3 eV).[1,11]

In model I and model II, the distance between the two graphite layers has been fixed at 3.4 Å. Usually, the irradiated-graphite specimen expands in the $c$ direction, which is induced by the large interstitial clusters formed within the interlayer space. The interlayer distance is enlarged accordingly. With the increase of the interlayer distance, the migration barrier from $B_i$ to $C_i$ will increase accordingly and approach the corresponding barrier through a graphene sheet.

For the diffusion along the $a$ axis, first, the interstitial must jump out of position A to position B, which will cost at least 1.2 eV energy. This is consistent with the calculation of Li *et al.*,[14] but deviates from the experiments which have shown that the migration energy should be less than 0.3 eV. My calculations show that the single interstitial could diffuse with the barrier less than 0.5 eV among structures B and C, which is close to the experimental results. So the question is whether all the single interstitials occupy position A in reality and remain at this state. A large number of experiments have observed that single interstitials could form large clusters.[7] These large clusters would enlarge the interlayer distance, which reduces the probability of occurrence of structure A. Defects may also induce shears in graphite and so may alter the local stacking order.[33] In the environment with other stacking orders, interstitials may not prefer to form so much strong bonds with graphite layers as structure A in the *AB*-stacking graphite. So the high migration energy from A to B in the *AB*-stacking graphite could be avoided. My calculations show that the interstitial migration energy in the *AA*-stacking graphite could decrease to 0.7 eV.

The behavior of defects in carbon nanotubes, fullerenes, and carbon onions has also intrigued much interest. Due to the curved walls of these materials, the behavior of the interstitial should be asymmetrical with respect to the curved walls. It will be easier for an interstitial to escape outward the nanotube, fullerene, or onion than to penetrate inward.

## IV. SUMMARY

In conclusion, a different migration path for the single carbon interstitial to penetrate the graphite layer is found, along which the migration energy is less than 0.5 eV. The migration energy along the $c$ axis is comparable to that along the $a$ axis. This finding is very important for the study of the irradiation effect in graphite and carbon nanotubes. The shear induced by the defects could reduce the interstitial migration energy.

## ACKNOWLEDGMENTS

This research has been supported by the Academy of Finland Centre of Excellence Program (2000–2005) and partially by the ELENA project within the Academy of Finland TULE programme. I am grateful to the Centre of Scientific Computing, Espoo, for computational resources. I thank A. S. Foster, A. V. Krasheninnikov, and R. M. Nieminen for useful discussions.

*yuma@uos.de

[1] F. Banhart, Rep. Prog. Phys. **62**, 1181 (1999).
[2] F. Banhart and P. M. Ajayan, Nature (London) **382**, 433 (1996).
[3] L. Sun, F. Banhart, A. V. Krasheninnikov, J. A. Rodríguez-Manzo, M. Terrones, and P. M. Ajayan, Science **312**, 1199 (2006).
[4] F. Banhart, T. Füller, P. Redlich, and P. M. Ajayan, Chem. Phys. Lett. **269**, 349 (1997).
[5] A. Hashimoto, K. Suenaga, A. Gloter, K. Urita, and S. Iijima, Nature (London) **430**, 870 (2004).
[6] E. Asari, M. Kitajima, K. G. Nakamura, and T. Kawabe, Phys. Rev. B **47**, 11143 (1993).
[7] K. Niwase, Phys. Rev. B **52**, 15785 (1995).
[8] K. Niwase, Phys. Rev. B **56**, 5685 (1997).
[9] F. Banhart, J. X. Li, and A. V. Krasheninnikov, Phys. Rev. B **71**, 241408(R) (2005).
[10] K. Urita, K. Suenaga, T. Sugai, H. Shinohara, and S. Iijima, Phys. Rev. Lett. **94**, 155502 (2005).
[11] C. H. Xu, C. L. Fu, and D. F. Pedraza, Phys. Rev. B **48**, 13273 (1993).
[12] P. O. Lehtinen, A. S. Foster, A. Ayuela, A. Krasheninnikov, K. Nordlund, and R. M. Nieminen, Phys. Rev. Lett. **91**, 017202 (2003).
[13] P. A. Thrower and R. M. Mayer, Phys. Status Solidi A **47**, 11 (1978).
[14] L. Li, S. Reich, and J. Robertson, Phys. Rev. B **72**, 184109 (2005).
[15] M. Hasegawa and K. Nishidate, Phys. Rev. B **70**, 205431 (2004).
[16] G. Kern and J. Hafner, Phys. Rev. B **58**, 13167 (1998).
[17] H. Rydberg, M. Dion, N. Jacobson, E. Schröder, P. Hyldgaard, S. I. Simak, D. C. Langreth, and B. I. Lundqvist, Phys. Rev. Lett. **91**, 126402 (2003).
[18] M. Elstner, P. Hobza, T. Frauenheim, S. Suhai, and E. Kaxiras, J. Chem. Phys. **114**, 5149 (2001).
[19] Q. Wu and W. Yang, J. Chem. Phys. **116**, 515 (2001).
[20] U. Zimmerli, M. Parrinello, and P. Koumoutsakos, J. Chem. Phys. **120**, 2693 (2004).
[21] A. J. Du and S. C. Smith, Nanotechnology **16**, 2118 (2005).
[22] G. Kresse and J. Furthmüller, Comput. Mater. Sci. **6**, 15 (1996).
[23] G. Kresse and J. Furthmüller, Phys. Rev. B **54**, 11169 (1996).
[24] J. P. Perdew, J. A. Chevary, S. H. Vosko, K. A. Jackson, M. R. Pederson, D. J. Singh, and C. Fiolhais, Phys. Rev. B **46**, 6671 (1992).
[25] G. Kresse and D. Joubert, Phys. Rev. B **59**, 1758 (1999).
[26] P. E. Blöchl, Phys. Rev. B **50**, 17953 (1994).
[27] Y. Baskin and L. Meyer, Phys. Rev. **100**, 544 (1955).
[28] M. T. Yin and M. L. Cohen, Phys. Rev. B **29**, 6996 (1984).
[29] L. X. Benedict, N. G. Chopra, M. L. Cohen, A. Zettl, S. G. Louie, and V. H. Crespi, Chem. Phys. Lett. **286**, 490 (1998).
[30] R. Zacharia, H. Ulbricht, and T. Hertel, Phys. Rev. B **69**, 155406 (2004).
[31] O. L. Blakslee, D. G. Proctor, E. J. Seldin, G. B. Spence, and T. Weng, J. Appl. Phys. **41**, 3373 (1970).
[32] G. Mills, H. Jonsson, and G. K. Schenter, Surf. Sci. **324**, 305 (1995).
[33] R. H. Telling, C. P. Ewels, A. A. El-Barbary, and M. I. Heggie, Nat. Mater. **2**, 333 (2003).